CrossMark
click for updates

Trypanosoma brucei RRM1 Is a Nuclear RNA-Binding Protein and Modulator of Chromatin Structure

Arunasalam Naguleswaran,[a] Kapila Gunasekera,[a] Bernd Schimanski,[a] Manfred Heller,[b] Andrew Hemphill,[c] Torsten Ochsenreiter,[a] Isabel Roditi[a]

Institute of Cell Biology, University of Bern, Bern, Switzerland[a]; Department of Clinical Research, University of Bern, Bern, Switzerland[b]; Vetsuissse Faculty, Institute of Parasitology, Bern, Switzerland[c]

ABSTRACT   TbRRM1 of *Trypanosoma brucei* is a nucleoprotein that was previously identified in a search for splicing factors in *T. brucei*. We show that TbRRM1 associates with mRNAs and with the auxiliary splicing factor polypyrimidine tract-binding protein 2, but not with components of the core spliceosome. TbRRM1 also interacts with several retrotransposon hot spot (RHS) proteins and histones. RNA immunoprecipitation of a tagged form of TbRRM1 from procyclic (insect) form trypanosomes identified ca. 1,500 transcripts that were enriched and 3,000 transcripts that were underrepresented compared to cellular mRNA. Enriched transcripts encoded RNA-binding proteins, including TbRRM1 itself, several RHS transcripts, mRNAs with long coding regions, and a high proportion of stage-regulated mRNAs that are more highly expressed in bloodstream forms. Transcripts encoding ribosomal proteins, other factors involved in translation, and procyclic-specific transcripts were underrepresented. Knockdown of TbRRM1 by RNA interference caused widespread changes in mRNA abundance, but these changes did not correlate with the binding of the protein to transcripts, and most splice sites were unchanged, negating a general role for TbRRM1 in splice site selection. When changes in mRNA abundance were mapped across the genome, regions with many downregulated mRNAs were identified. Two regions were analyzed by chromatin immunoprecipitation, both of which exhibited increases in nucleosome occupancy upon TbRRM1 depletion. In addition, subjecting cells to heat shock resulted in translocation of TbRRM1 to the cytoplasm and compaction of chromatin, consistent with a second role for TbRRM1 in modulating chromatin structure.

IMPORTANCE   *Trypanosoma brucei*, the parasite that causes human sleeping sickness, is transmitted by tsetse flies. The parasite progresses through different life cycle stages in its two hosts, altering its pattern of gene expression in the process. In trypanosomes, protein-coding genes are organized as polycistronic units that are processed into monocistronic mRNAs. Since genes in the same unit can be regulated independently of each other, it is believed that gene regulation is essentially posttranscriptional. In this study, we investigated the role of a nuclear RNA-binding protein, TbRRM1, in the insect stage of the parasite. We found that TbRRM1 binds nuclear mRNAs and also affects chromatin status. Reduction of nuclear TbRRM1 by RNA interference or heat shock resulted in chromatin compaction. We propose that TbRRM1 regulates RNA polymerase II-driven gene expression both cotranscriptionally, by facilitating transcription and efficient splicing, and posttranscriptionally, via its interaction with nuclear mRNAs.

Polycistronic transcription is a hallmark of unicellular eukaryotes known as kinetoplastids, which include the TriTryps *Trypanosoma brucei*, *Leishmania major*, and *Trypanosoma cruzi*. Precursor RNAs that can span scores of genes are subsequently processed into monocistronic mRNAs flanked by a 5′ spliced leader and a poly(A) tail (recently reviewed in references 1, 2, and 3). Following transcription and processing, the mRNAs derived from adjacent genes in a polycistronic transcription unit are regulated autonomously, and their relative abundance can differ by orders of magnitude. Steady-state mRNA levels can be regulated by alterations in RNA processing efficiency (4, 5) or RNA stability (6). Moreover, the stability of individual transcripts can change in response to external signals, such as temperature (7) or the presence of simple metabolites in the culture medium (8, 9). mRNA levels are not necessarily an accurate reflection of protein levels, with translation providing an additional layer of control (10, 11). Taken together, this has led to the concept of posttranscriptional regulons; the genes belonging to a regulon might be dispersed throughout the genome, but they are coordinately regulated at particular phases of the life cycle, the cell cycle, or in response to external signals (12–15). Implicit in this model are a series of protein factors that mediate their control by binding to elements on pre-RNAs or mature mRNAs.

There is compelling evidence that chromatin structure also contributes to regulation in trypanosomes. The transcription units encoding the variant surface glycoprotein (VSG) of blood-

stream forms and the procyclins in insect midgut (procyclic) forms are transcribed by RNA polymerase I (16–18), the former in the nuclear expression site body (19) and the latter in the nucleolus (20). The active VSG expression site in bloodstream forms and the procyclin expression site in insect forms are depleted of nucleosomes. Silent VSG expression sites have greater nucleosome occupancy than the active site and are activated upon depletion of chromatin remodeling factors (21–23). A landmark study by Siegel et al. (24) showed that RNA polymerase II transcription start sites are marked by specific histone modifications and incorporation of histone variants, such as H2AZ and H2BV (24). This creates an open chromatin structure that enables the transcription machinery to bind and initiate transcription. In other eukaryotes, transcription, splicing, and chromatin remodeling are coupled and can regulate each other (25, 26). This is mediated through specific epigenetic marks on histones (27–29), localized action of histone remodelers (30), and specific recruitment of auxiliary splicing factors, including SR family proteins (31–33). *T. brucei* possesses at least two SR proteins, TbRRM1 (Tb927.2.4710) and TSR1 (Tb927.8.900), which were identified independently (34, 35). TSR1 has recently been shown to modulate the splicing of a subset of transcripts and is considered an auxiliary factor in this process (36). In addition, three more SR proteins are predicted to be encoded in the genome (RBSR1 [Tb927.9.6870], RBSR2 [Tb927.7.1390], and RBSR3 [Tb927.3.5460]). In other organisms, SR proteins can integrate transcription with chromatin conformation by binding nascent RNA. This constitutes a platform to which they recruit the RNA processing machinery as well as creating permissive chromatin to facilitate transcription elongation by RNA polymerase II (37).

In this study, we investigated the role of TbRRM1 in regulating gene expression in *T. brucei*. We found that, in procyclic forms, ribonucleoprotein complexes containing TbRRM1 are enriched for certain subsets of mRNAs, including many that are preferentially expressed in bloodstream forms, while procyclic-specific mRNAs are underrepresented. TbRRM1 is found in complex(es) with a known auxiliary splicing factor, polypyrimidine tract-binding protein 2 (PTB2) (5), several retrotransposon hot spot (RHS) proteins, and histones. Depletion of TbRRM1 results in major changes to the transcriptome, concomitant with increased nucleosome occupancy in specific regions of the genome. Heat shock induces translocation of RRM1 from the nucleus to the cytoplasm and also results in chromatin tightening, suggesting a second role for RRM1 as a chromatin modulator.

RESULTS

TbRRM1 exhibits positive and negative selectivity toward mRNAs. TbRRM1 is a nucleoprotein that was identified 16 years ago in a search for factors involved in *trans*-splicing (34). The polypeptide contains 3 RNA recognition motifs (RRMs), 2 zinc finger domains, and an arginine/serine-rich domain. It was shown previously that conditional knockout of RRM1 perturbed cell division and resulted in decreased incorporation of radiolabeled UTP or orthophosphate into RNA (34, 38). The transcription of the spliced leader and its utilization were unchanged, however, and there were no qualitative differences in small RNAs (38). From these results, it was concluded that TbRRM1 did not have a general role in splicing. Moreover, the protein was not identified in the core spliceosome (39, 40).

To determine if mRNAs interact directly with TbRRM1, we generated a cell line that exclusively expressed a hemagglutinin (HA)-tagged version of the protein for use in RNA immunoprecipitation (RIP). To achieve this, one allele was replaced by a hygromycin resistance cassette, and the second allele was tagged *in situ* at the N terminus. These cells grew normally, indicating that the tagged version of TbRRM1 was functional. The localization of HA-RRM1 was monitored in an immunofluorescence assay (see Fig. S1A in the supplemental material), which confirmed that the tagged protein shared the same nuclear localization as the wild-type protein. To isolate transcripts bound to TbRRM1, RIP was performed with an HA-affinity matrix. Wild-type cells were processed in parallel as a negative control. Following DNase treatment to remove contaminating genomic DNA, reverse transcription-PCR (RT-PCR) was performed with primer pairs for transcripts encoding procyclins, β-tubulin, actin, and the ribosomal proteins RPL10 and RPL30. For each pair of primers, total RNA and a reaction without reverse transcriptase were included as positive and negative controls, respectively. The RIP sample from the HA-tagged TbRRM1 cell line gave products for all primer sets; no products were amplified from the wild-type control, confirming the specificity of the pulldown (see Fig. S1B).

To gain further information about the mRNAs associated with RRM1, we performed RIP followed by next-generation sequencing (RIP-Seq). Enrichment ratios were calculated relative to the tags obtained with mRNA from the same cell line. This revealed sets of RNAs that were enriched ≥2-fold or underrepresented in the RIP sample (Fig. 1A; see also Tables S1A and B in the supplemental material). Additional analysis revealed that there was an inverse correlation between cellular mRNA abundance and enrichment after RIP (Fig. 1B). In addition, longer transcripts were more likely to be enriched than were shorter transcripts (Fig. 1C).

Of the 1,500 transcripts that were enriched, many encoded RNA-binding proteins. The most highly enriched transcript was RBP26 (95-fold enrichment); the transcript for RRM1 itself was enriched 10-fold, and the bloodstream-specific RBP10 was enriched 58-fold (41). In addition, 7 out of 11 transcripts encoding PUF proteins were enriched >8-fold. Other notable categories among the enriched transcripts were those encoding retrotransposon hot spot proteins (2- to 31-fold increases [42]) and transcripts with long coding regions in excess of 9 kb, such as antigenic protein (31-fold), dynein heavy chains (2- to 8-fold enrichment), and hydin (6.4-fold). In addition, 153 novel transcripts were enriched between 2- and 76-fold. More than 15% of enriched transcripts were previously identified to be more abundant in bloodstream forms than salivary gland forms (see Table S1C in the supplemental material) (43). Other bloodstream-form-specific mRNAs included alternative oxidase (44), the haptoglobin-hemoglobin receptor (45), and invariant surface glycoproteins (ISG75) (46). In addition, 15 transcripts that are upregulated in salivary gland trypanosomes, including BARP (47), were identified (see Table S1C) (43). Interestingly, specific categories of transcripts were underrepresented in the RIP samples. Of 3,000 underrepresented transcripts (11% of them more than 10-fold decreased), the most striking category was that of ribosomal proteins, levels of which ranged from 10- to 72-fold lower than in the input RNA. Transcripts encoding translation initiation factors and other proteins implicated in translation, including all four Alba domain proteins (48), were also underrepresented. Interestingly, procyclic-stage-specific mRNAs were underrepresented. These included the EP procyclins (≥14-fold) (49), PSSA-2 (7.9-
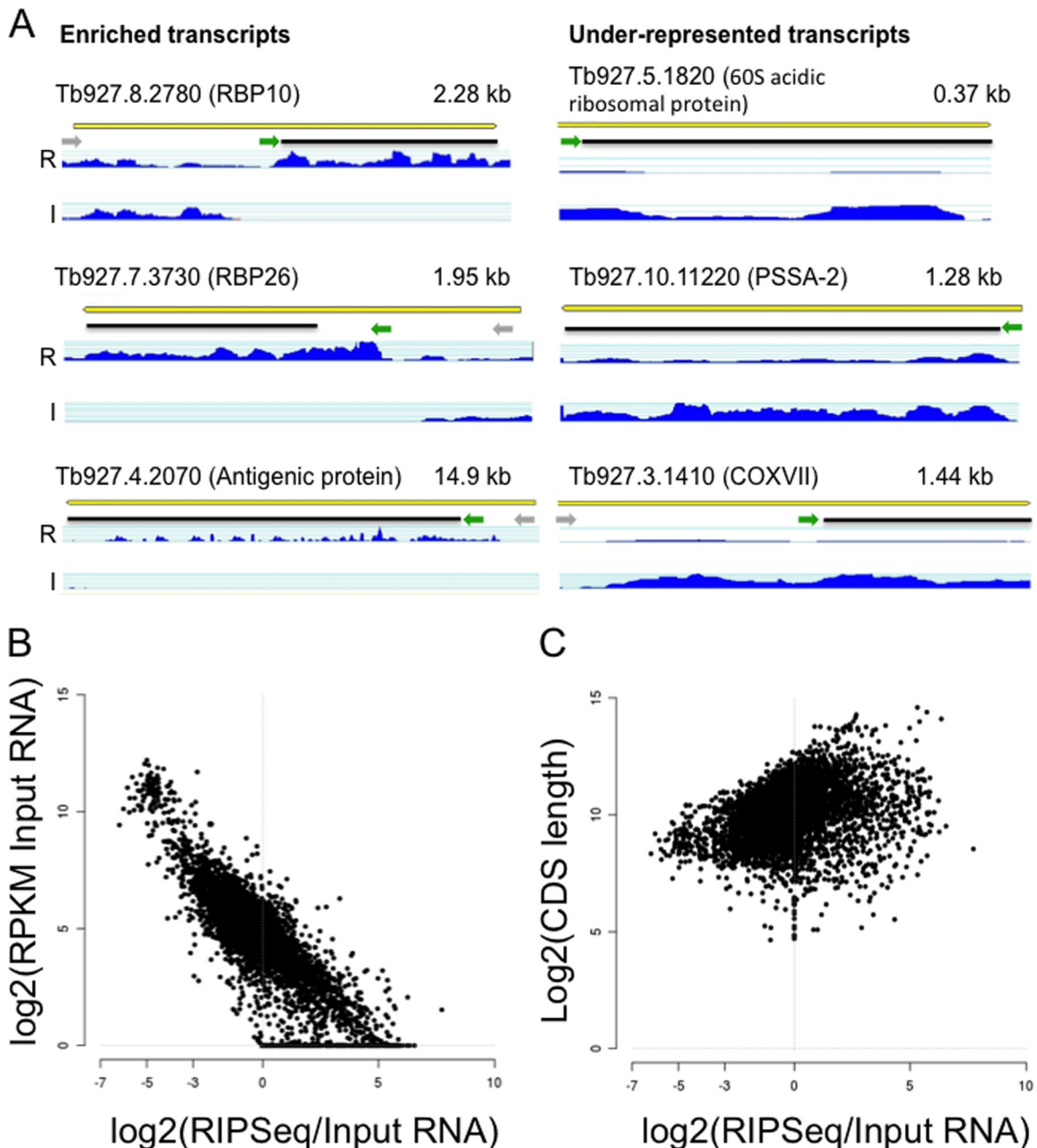
FIG 1 (A) Examples of enriched and underrepresented transcripts after RIP. Read densities of samples from RIP-Seq with HA-RRM1 (R) and total mRNA (I) were compared. Genes as defined in TriTrypDB are depicted by the yellow bars; their lengths are given in kilobases. ORF are shown as black bars. Major splice sites are depicted by green arrows, and minor splice sites are shown as gray arrows. For each example, the scales for R (RIP-Seq) and I (input) are the same (read density in tags per million) but were adjusted to different maximum tag numbers. The maxima were as follows: RBP10, 436; RBP26, 791; antigenic protein, 6,447; 60S acidic ribosomal protein, 5,664; PSSA-2, 1,754; COXVII, 2,914. (B) Inverse correlation between enrichment after RIP relative to input mRNA (*x* axis) and mRNA abundance in the input sample (*y* axis). (C) Relationship between the length of mRNA coding regions (CDs) and enrichment after RIP relative to input mRNA. Note that the lengths of 5′ and 3′ untranslated regions were not taken into account.

fold) (50), and numerous mRNAs encoding mitochondrial proteins, for example, cytochrome oxidase subunits V to IX (>10-fold) (51).

Interaction partners of TbRRM1. To shed further light on the biological role(s) of TbRRM1, we used the HA-RRM1 cell line to isolate protein complexes. Proteins were cross-linked *in vivo* with 0.1% paraformaldehyde and enriched with an HA-affinity matrix. As a negative control, the same procedure was performed with wild-type cells. Proteins were separated by SDS-PAGE, and major bands specific to the HA-RRM1 line were subjected to liquid chromatography-mass spectrometry (LC-MS) (see Fig. S2 in the supplemental material). This led to the identification of the RNA-binding proteins RRM2 (Tb927.6.2550) and PTB2/DRDB4 (Tb927.11.14100) and the nucleolar RNA helicase II (Tb927. 5.4420). PTB2/DRDB4 has previously been implicated in splicing of a subset of transcripts (5), which would be consistent with a role
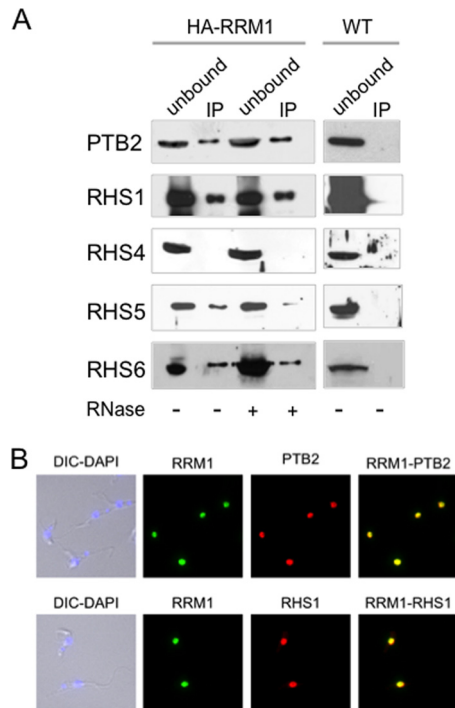
FIG 2 Proteins that interact with HA-RRM1. (A) Protein complexes were purified using an anti-HA affinity matrix, with (+) or without (−) prior treatment of the lysates with RNase A. Unbound and immunoprecipitated (IP) proteins were analyzed by Western blotting. Twice as many cell equivalents were loaded for the IP proteins than for unbound proteins. (B) Colocalization of RRM1 with PTB2 and RHS1 in the nucleus. Information about the different antibodies is given in the supplemental material.
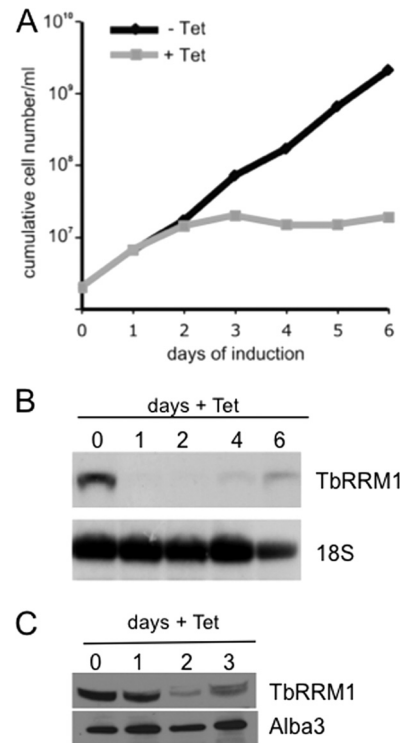

FIG 3 Effect of RNAi against TbRRM1. A stem-loop construct covering the coding region of TbRRM1 was integrated into the ribosomal spacer in procyclic forms of AnTat 90-13. (A) Growth of an uninduced culture (-Tet) or culture induced with tetracycline (+Tet) over a period of 6 days. (B) Northern blot analysis results with TbRRM1 transcript samples during the time course. 18S rRNA was used as a loading control. (C) Western blot analysis results with TbRRM1 following induction of RNAi.

for TbRRM1 in mRNA processing. We also identified three families of retrotransposon hot spot proteins, RHS1, -4, and -5, which are mainly concentrated in the nucleus (42), and core histones. Interactions with PTB2, RHS1, RHS5, and RHS6 were confirmed by immunoprecipitation and Western blot analysis (Fig. 2A). In addition, colocalization of RRM1 with PTB2 and RHS1 was demonstrated (Fig. 2B). Treatment with RNase A had no effect on any of these interactions, indicating that they were not RNA dependent. Although RHS4 was clearly identified by mass spectrometry (7 unique peptides), it was not detected after immunoprecipitation; the reasons for this are unknown. Other proteins that were identified by mass spectrometry were tubulins and mitochondrial and cytoplasmic HSP70 (which are common contaminants of such preparations). We could not confirm interactions between TbRRM1 and either mitochondrial or cytoplasmic HSP70 by immunoprecipitation and Western blotting, however (data not shown).

Wide-ranging effects of TbRRM1 depletion on mRNA abundance. To further analyze the role of TbRRM1, an RNA interference (RNAi) line was generated in procyclic forms of AnTat 90-13. As reported by Manger and Boothroyd (38), depletion of TbRRM1 led to growth arrest, starting on day 3 (Fig. 3A). Western blot analysis showed TbRRM1 was at its lowest level on day 2. We therefore chose day 2 for analysis of the transcriptome. To evaluate the absolute levels of mature mRNA upon TbRRM1 depletion, we hybridized a Northern blot with an antisense probe against the spliced leader (52). There was no significant difference in the

amount of mature mRNA between uninduced and induced cells (data not shown).

To assess the effect of depleting TbRRM1 on the transcriptome as a whole, a variant of RNA-Seq, known as spliced leader trapping (SLT) (53), was performed with mRNA from uninduced cells (RRM−) and cells 2 day postinduction (RRM+). This technique, which utilizes the spliced leader sequence as a sequencing primer, simultaneously identifies splice acceptor sites and measures mRNA abundance based on the number of tags. *T. brucei* encodes 12,094 genes (TriTrypDB version 5.2). Comparison of the normalized gene expression profiles (Fig. 4) revealed profound differences in mRNA abundance, with 4,369 transcripts showing a ≥2-fold decrease in splice leader tags ($P \leq 10^{-5}$) in cells depleted of RRM1; of these, 231 transcripts decreased ≥10-fold. Approximately 300 transcripts showed a ≥2-fold increase ($P \leq 10^{-5}$) (Fig. 4; see also Tables S2A and B in the supplemental material). Following induction, there was a 9-fold decrease in tags mapping to TbRRM1, confirming successful knockdown. In agreement with Manger and Boothroyd (38), we did not find alterations in the overall level of the spliced leader precursor (data not shown), but instead we found that polyadenylated forms of the precursor were increased (Fig. 6A, Chr 9). This accumulation was confirmed by quantitative PCR (qPCR) (data not shown). It has been shown that polyadenylated spliced leader precursors accumulate in stumpy forms, which are quiescent, and this may be a means of turning off mRNA production (54). Based on GO term analysis,
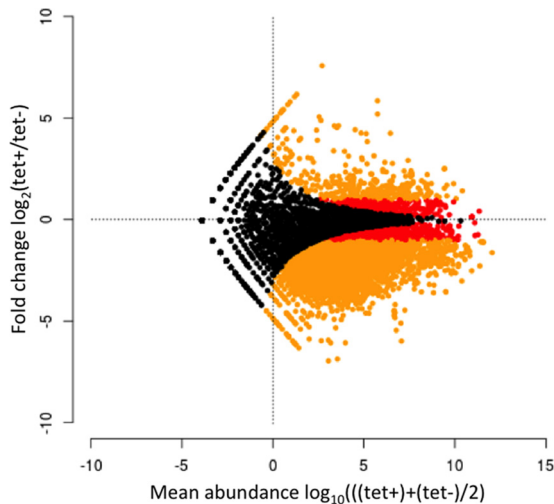
FIG 4 Changes in spliced leader tags 2 days postinduction of RNAi against TbRRM1. The scatter plot is based on the mean SLT abundance (*x* axis) and fold change in $\log_2$ SLT abundance (*y* axis). The red circles indicate genes with significantly changed transcript abundance levels, based on a *P* value of $\leq 10^{-5}$, but with changes <2-fold; orange circles indicate SLT tags changed $\geq$2-fold and with a *P* value of $\leq 10^{-5}$.
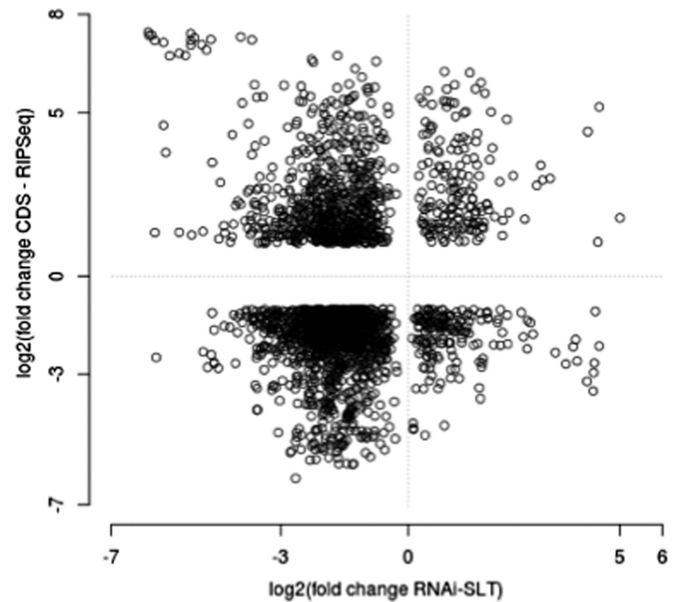

FIG 5 Lack of correlation between the association with TbRRM1 and changes in spliced leader tags following RNAi. Transcripts from RIP-Seq that were either enriched $\geq$2-fold or underrepresented 2-fold compared to input mRNA were plotted against transcripts that were significantly regulated upon RRM1 knockdown. Correlation values were as follows: Spearman's rank correlation, $R = 0.03473595$ and $P = 0.08861$; Pearson's product-moment correlation, $R = 0.02334118$ and $P = 0.2526$.

we could not identify categories of genes that were preferentially regulated. When the positions of splice sites were analyzed, 96% remained unchanged, but a number of examples of increased expression mapped either to internal sites (e.g., Tb927.9.8340) or to upstream sites that encompassed additional short open reading frames (ORF) before the major ORF (e.g., Tb927.11.12130). However, there were also increases in bona fide transcripts encoding RNA-binding proteins, a putative nucleosome assembly protein, and kinases (see Table S2B in the supplemental material), all of which could conceivably exert secondary effects on the transcriptome.

There was no correlation between the ability of a transcript to associate with TbRRM1 and changes in abundance following RNAi (Fig. 5). Transcripts showing the greatest increases in abundance after knockdown of TbRRM1 were neither selectively enriched nor underrepresented in the RIP-Seq. Tags for RBP26, the most highly enriched transcript in RIP-Seq, decreased <2-fold after RNAi. An array of five glucose transporters, which were underrepresented in RIP-Seq and thus might be independent of TbRRM1, showed a >20-fold reduction in tags.

Depletion of RRM1 leads to changes in histone occupancy. The changes in transcript levels observed after RNAi were mapped to the whole genome. This revealed large regions of downregulated genes on all 11 chromosomes (see Fig. S3 in the supplemental material). One means of reducing gene expression is by tightening chromatin structure. For example, silent VSG expression sites in bloodstream-form trypanosomes show much greater histone occupancy than the transcriptionally active VSG expression site (21–23). To see if histone occupancy was altered after RRM1 knockdown, we performed chromatin immunoprecipitation (ChIP) with an anti-histone H3 antibody, followed by qPCR on regions of chromosome 4 (Chr 4) and Chr 9, in which the majority of genes were downregulated and no genes were upregulated (Fig. 6A). As shown in Fig. 6B, histone occupancy increased in these regions when TbRRM1 was knocked down, although total levels of his-

tone H3 protein did not change (Fig. 6D). No significant changes in histone occupancy were observed for housekeeping genes, such as α-tubulin and ribosomal proteins L10 (Tb927.11.9710) and L30 (Tb927.10.4110), whose transcript levels were not dependent on TbRRM1 (Fig. 6C). To obtain more information on bulk chromatin structure, we performed transmission electron microscopy on cells from the TbRRM1 RNAi clone. Two days after induction of RNAi, there was substantially more heterochromatin than found in the nuclei of uninduced cells (Fig. 7A). Immunofluorescent labeling with the nucleolar marker L1C6 showed that this was not due to a change in the diameter of the nucleolus upon depletion of TbRRM1 (Tet−, 682 ± 148 nm; Tet+, 652 ± 124 nm, respectively [means ± standard deviations of the means]) (see Fig. S4A in the supplemental material).

The results reported above indicate that TbRRM1 can influence chromatin structure, but they do not establish whether the effect is direct or indirect. We therefore performed immunoprecipitation of HA-RRM1 and probed for the presence of histone H3 (Fig. 7B). H3 was detected in association with TbRRM1 when lysates were treated with RNase A prior to the incubation with HA-matrix; although they were not detected in untreated lysates under these exposure conditions, faint bands could be seen when the blot was overexposed (see Fig. S4B in the supplemental material). These results show, first, that TbRRM1 is capable of interacting with histones and, second, that the connection is not an indirect one via an RNA bridge.

Heat shock alters the localization of TbRRM1 and results in chromatin condensation. Under normal culture conditions, TbRRM1 is localized throughout the nucleus. However, several mRNA processing factors have been reported to translocate to nuclear speckles when cells are subjected to heat shock, or they
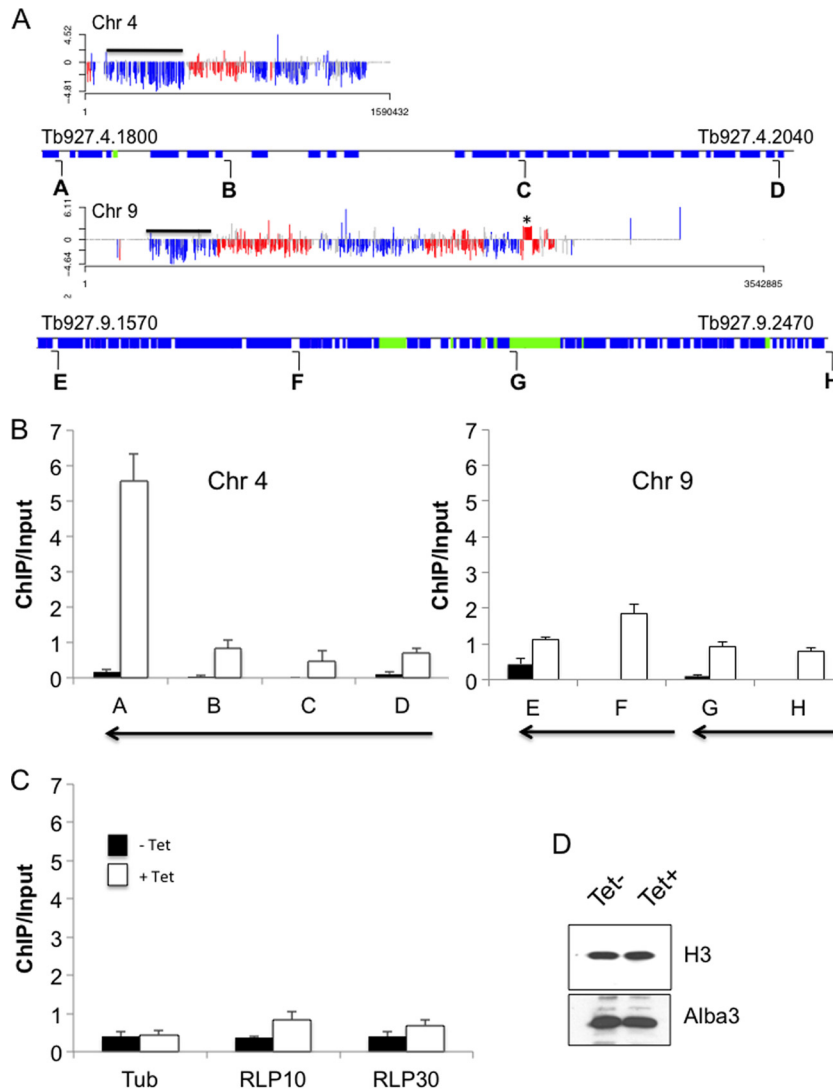
FIG 6 Effect of RNAi against TbRRM1 on histone occupancy on selected regions of chromosome 4 (Chr 4) and Chr 9. (A) Changes in transcript abundance (fold changes) across chromosomes 4 and 9 after RNAi. The region on chromosome 9 encoding the spliced leader precursors is marked by an asterisk. The regions marked by black lines are enlarged below the chromosomes. Coding regions are shown as blue rectangles, and novel transcripts are shown as green rectangles. Gene IDs are given for the first and last genes in these regions. The vertical bars along each chromosome represent the difference in abundance ($\log_2$). The red and blue colors indicate the sense and antisense strands, respectively. The same colors also indicate the transcripts that are significantly different in abundance. Gray bars indicate transcripts that do not change significantly in abundance ($P \leq 10^{-5}$). Empty spaces denote regions where no reads were mapped (for example, telomeres) or there was no detectable change in abundance. (B) Anti-histone H3 ChIP analysis was performed across two clusters on chromosomes 4 and 9 (marked by black bars in panel A). Primer sequences are given in the supplemental material, and their positions in the genome are shown below each chromosome in panel A. Tet−, TbRRM1 RNAi clone without induction of double-stranded RNA; Tet+ TbRRM1 RNAi clone after a 2-day induction with tetracycline. Black arrows indicate the direction of transcription. (C) Anti-histone H3 ChIP analysis results with the three housekeeping genes. These genes were selected because RNAi against TbRRM1 did not affect the steady-state levels of the mature RNAs. The same genes were used to normalize SLT data (D) Western blot showing that histone H3 levels remained unchanged during RNAi. Alba3 was used as a loading control.

may be found in the cytoplasm when cells are subjected to transcription inhibition (55, 56). Heat shock is known to inhibit transcription in trypanosomes (57). We therefore tested its effect on the localization of TbRRM1. In procyclic forms subjected to severe heat shock (41°C for 1 h, according to the methods described in reference 52), TbRRM1 translocated from the nucleus to the cytoplasm (Fig. 8). Following recovery at 27°C for 1 h after heat shock, TbRRM1 reaccumulated in the nucleus in close to 100% of the cells. Translocation from the nucleus to the cytoplasm did not occur in the presence of leptomycin B, an inhibitor of exportin I-mediated nuclear export, indicating that it was due to an active process rather than nonspecific permeability of the nuclear membrane. We also tested the effects of genotoxic stress, transcription arrest, translation inhibition, starvation, osmotic stress, and endoplasmic reticulum (ER) stress, but none of these resulted in movement of TbRRM1 (data not shown). Thus, translocation of TbRRM1 from the nucleus to the cytoplasm may be part of a specific heat shock response that tightens chromatin. To test this hypothesis, we performed ChIP for histone occupancy changes upon heat shock. Our data demonstrated that there is a general
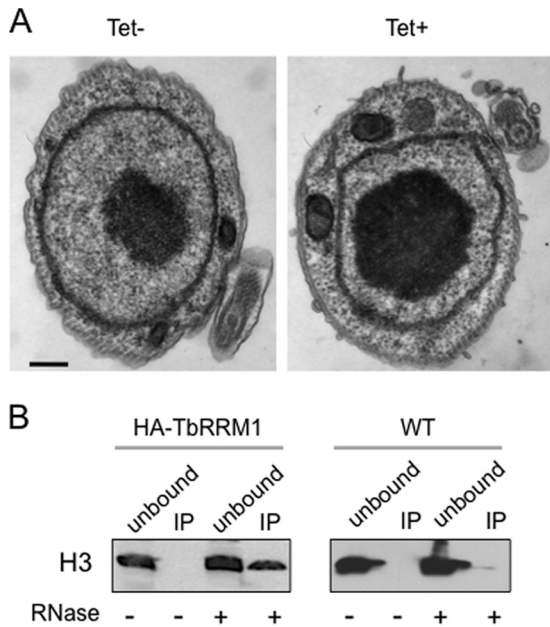
FIG 7 TbRRM1 interactions with histones and the effect of its depletion on heterochromatin. (A) Electron micrographs showing representative cross-sections though nuclei of cells without induction of RNAi (left) or after 2 days of induction with tetracycline (right). An increase in heterochromatin was apparent after RNAi. Bar, 0.25 μm. (B) The interaction of histone H3 with HA-RRM1 is enhanced by RNase treatment. HA-RRM1 was purified from cell lysates with or without prior treatment with RNase A. Samples were analyzed by Western blotting. Twice as many cell equivalents were loaded for the immunoprecipitated sample (IP) compared to unbound sample.
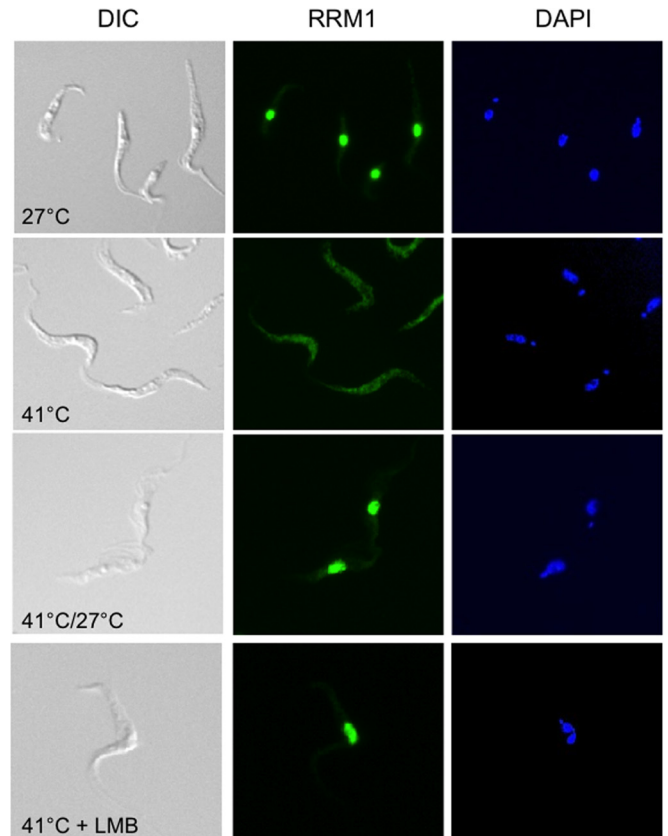
FIG 8 Effect of heat shock on localization of TbRRM1. The columns, from left to right, show differential interference contrast (DIC) images, samples stained with RRM1 antibody, and samples stained with DAPI. Under normal culture conditions at 27°C, TbRRM1 localizes to the nucleus. Other experimental conditions: 41°C, transfer of culture to 41°C for 1 h; 41°C/27°C, heat shock for 1 h followed by recovery at 27°C for 1 h; LMB, addition of 10 nM leptomycin B immediately prior to heat shock. TbRRM1 was detected with anti-HA antibody.

increase of histone occupancy in the regions we investigated (see Fig. S5 in the supplemental material). Collectively, our data from TbRRM1 depletion and heat shock studies indicate that the protein may play a role in maintaining permissive chromatin in *T. brucei* to facilitate transcription and RNA processing.

DISCUSSION

SR proteins in higher eukaryotes have multiple functions in transcription, RNA processing, RNA export, and control of stability (58). Importantly, they can link transcription to chromatin structure by binding nascent RNA and recruiting chromatin modifiers (37). Our studies showed that the nucleoprotein TbRRM1 is likely to fulfill a similar role, as it binds nuclear mRNA and modulates chromatin structure in *T. brucei*. Based on its domain structure, the protein was originally classified as a putative splicing factor (34). We demonstrated that it associates with the auxiliary splicing factor PTB2, RRM2, several RHS proteins, and histones, but not with components of the core spliceosome. Data from Manger and Boothroyd (38) and our analysis (data not shown) indicated that TbRRM1 does not play a global role in *trans*-splicing. However, given its association with PTB2, we cannot exclude that TbRRM1 functions in splicing commitment for a subset of transcripts, analogous to some SR splicing factors in mammals and TSR1 in *T. brucei* (36).

Isolation of messenger ribonucleoproteins containing a functional tagged form of TbRRM1 from procyclic trypanosomes showed its association with most mRNAs, but also revealed both positive and negative selectivity. It is striking that stage-specific transcripts from procyclic forms, such as those encoding surface

proteins (procyclins and PSSA-2), and nuclear-encoded mitochondrial proteins were underrepresented in the RIP sample, whereas transcripts that are upregulated in bloodstream forms and salivary gland forms were enriched. Given that TbRRM1 binds most mRNAs, at its simplest this may reflect the differences between the population of newly synthesized mRNA in the nucleus and the bulk mRNA in the cell. This would also be consistent with the observation that mRNAs of low abundance are preferentially associated with TbRRM1, since mRNAs from "inappropriate" life cycle stages can still be transcribed, but they would be degraded more rapidly. Another function of TbRRM1 might be to retain these transcripts in the nucleus, thereby preventing their translation. For this to be a general function, however, TbRRM1 would need to recognize different transcripts depending on the life cycle stage. This might be achieved through association with different RHS proteins, some of which are also stage regulated (see Table S1C in the supplemental material). We searched for conserved motifs in a subset of enriched bloodstream-form-specific transcripts but, although U- and A-rich elements occurred fairly frequently, there were no obvious consensus sequences. We cannot rule out, however, that the secondary structure rather than the primary sequence determines the specificity. Another category of

enriched transcripts included mRNAs with long coding regions. It has been shown in other systems that long RNAs can interfere with transcription (59) and that these require active removal from the DNA template (58). Since the affinity of TbRRM1 is greater for RNA than for histones, one function might be to assist in displacing the nascent mRNA from the site of transcription. Selective loss of mRNAs with long coding regions has also been reported for trypanosomes depleted of PUF2, but this must operate by a different mechanism, since PUF2 is not found in the nucleus (60).

Knockdown of TbRRM1 by RNAi resulted in profound changes to the transcriptome, preceding the onset of growth arrest. Analysis of the affected transcripts did not reveal preferential changes in particular categories of genes, nor was there a correlation with enrichment or depletion based on RIP-Seq. Unraveling these changes is complex, however, as they might be primary or secondary effects of TbRRM1 depletion. Primary effects could be exerted on transcripts that use the protein as an auxiliary factor for splicing; secondary effects might occur with transcripts whose processing or turnover depends on RNA-binding proteins downstream of TbRRM1. At first sight, these numerous alterations to the transcriptome might appear to be at odds with the insignificant changes in the overall levels of spliced mRNAs (see Fig. S3 in the supplemental material). It should be borne in mind, however, that almost two-thirds of the transcriptome does not change and that many abundant transcripts, for example, α-tubulin, do not fluctuate.

It has been shown that depletion of PTB2 causes major changes to the transcriptome, particularly mRNAs with C-rich splice sites (5). Since TbRRM1 and PTB2 interact, we attempted to compare the data sets. This was complicated, however, since the analysis of PTB2 was performed with a different strain of *T. brucei* and using microarrays, while our analysis of TbRRM1 was by SLT. Nevertheless, as far as we can determine, the major changes detected by Stern and coworkers (5) are only partially reflected in our data set.

Several findings support an additional function for TbRRM1 in modulating chromatin structure. TbRRM1 interacts with histones, and nuclei depleted of TbRRM1 contain considerably more heterochromatin than their undepleted counterparts. This was confirmed by ChIP analysis, which revealed significant increases in histone occupancy in the two regions we examined on Chr 4 and Chr 9. Like SR proteins in other systems (56), TbRRM1 is able to relocalize in response to stress. Interestingly, it has been documented that genome organization plays a role in the heat shock response of *T. brucei*, with downregulated genes tending to be proximal to transcription start sites, while upregulated genes are more likely to be distal (57). This effect might be due, in part, to chromatin tightening in the absence of TbRRM1, preventing (re-)initiation of transcription. We also explored the possibility that TbRRM1 escorts specific transcripts to the cytoplasm for selective translation, but we were unable to detect its association with RNA after heat shock (data not shown).

In summary, our data demonstrate that in addition to being a nuclear RNA-binding protein, TbRRM1 also plays a role in regulating histone occupancy in at least two regions of the genome. Thus, it may operate at both posttranscriptional and transcriptional levels. While a correlation between chromatin structure and transcription has been demonstrated for RNA polymerase I in *T. brucei* (21–23), this remains to be explored for RNA polymerase II.

MATERIALS AND METHODS

Trypanosome strains and generation of mutants. *T. brucei* brucei AnTat 1.1 (61) and AnTat1.1 90-13 (7) were used in this study. Procyclic forms were cultured in SDM-79 (62) supplemented with 10% fetal bovine serum. Stable transformation was performed by electroporation according to established procedures (8). For inducible RNAi against RRM1, procyclic forms of AnTat1.1 90-13 (7) were transfected with NotI-linearized pRRM1-RNAi. The exclusive expresser HA-RRM1 was generated in AnTat 1.1 by deletion of one endogenous copy of RRM1, using the vector pRRM1-Hyg-KO, and replacement of the second endogenous copy by a HA-tagged form encoded by pHA-RRM1-puro. Information on the generation of constructs is provided in the supplemental material.

Northern and Western blot analyses. Isolation of total RNA with hot phenol (63), Northern blotting, hybridization, and detection were performed as described previously (64). For Western blot assays, protein samples were separated by denaturing SDS-PAGE gel electrophoresis and transferred onto polyvinylidene difluoride membranes by semidry blotting. The primary antibodies used in this study are listed in the supplemental material. Peroxidase-labeled secondary antibodies were diluted 1:5,000, and chemiluminescence was detected with the SuperSignal West Pico chemiluminescence substrate (Thermo Scientific).

Microscopy. (i) Fluorescence microscopy. For fluorescence microscopy, cells were washed with phosphate-buffered saline (PBS), allowed to adhere to coverslips at a density of 2×10^6 cells/ml, and fixed with 1% formaldehyde in PBS. After permeabilization with PBS–0.1% Triton X-100 and blocking with 3% bovine serum albumin in PBS, cells were incubated with monoclonal rat anti-HA 3F10 antibody (Roche) diluted 1:200 in blocking solution. As a secondary antibody, Alexa Fluor 594-conjugated goat anti-rat antibody (Invitrogen) was used after dilution to 1:2,000 in blocking solution. After the final washing steps, the samples were mounted in Vectashield containing 4′,6-diamidino-2-phenylindole (DAPI; Vector Laboratories). Images were made with a Leica DFC360FX monochrome charge-coupled-device camera mounted on a Leica dm5500 B microscope and analyzed using LAS AF software (Leica).

(ii) Transmission electron microscopy. For transmission electron microscopy, processing, fixation, and imaging were performed as described previously (65).

Isolation of ribonucleoprotein particles and mass spectrometry. Ribonucleoprotein particles were purified from cells expressing HA-RRM1 as described previously (66). For isolation of RNA bound to RRM1, anti-HA magnetic beads (Pierce) were used, and the RNA-protein complexes were resuspended in 20 mM Tris-HCl (pH 7.5), 5 mM EDTA, 50 mM NaCl, 0.1% SDS, and 50 μg/ml proteinase K and incubated at 70°C for 40 min. RNA was purified by phenol-chloroform extraction and ethanol precipitation, subjected to DNase treatment, and used for cDNA synthesis or RNA-Seq (Fasteris SA, Geneva, Switzerland). For isolation of proteins interacting with RRM1, the protein complexes were eluted from the anti-HA affinity matrix with 0.1 M glycine (pH 2.6) and immediately neutralized with 1 M Tris. Protein cross-linking was reversed by incubating the sample at 70°C for 40 min. Proteins were precipitated with methanol-chloroform (67) and subjected to Western blotting, or protein bands were cut from Coomassie-stained gels, subjected to trypsin digestion, and analyzed by LC-tandem MS (68).

cDNA synthesis, qPCR, SLT, and RNA-Seq. Reverse transcription was performed using a SuperScript RT II kit (Invitrogen) according to the manufacturer's instructions, with random hexamers as primers. The PCR primers used to analyze transcripts associated with RRM1 are reported in the supplemental material. qPCR was performed using MESA Green qPCR MasterMix Plus for SYBR assay (Eurogentec) in the ABI Prism 7000 sequence detection system (Applied Biosystems). The data were analyzed using 7000 System SDS software v1.2 (Applied Biosytems).

(i) Spliced leader trapping. SLT was performed as described previously, using mRNA derived from the rrm1 RNAi line, either uninduced (RRM1⁻) or incubated for 2 days with tetracycline (RRM1⁺). RNA ex-

traction and library construction (Fasteris SA, Geneva, Switzerland) were performed essentially as described elsewhere (69).

(ii) RNA immunoprecipitation followed by Illumina sequencing. RIP-Seq was performed at Fasteris (Geneva, Switzerland). Briefly, RIP RNA and input RNAs were subjected to the TruSeq stranded mRNA protocol (Illumina), which enables the analysis of expressed mRNAs and the orientation of the transcripts. To minimize rRNA contamination, input sample was oligo(dT) selected, whereas the RIP sample was converted directly into cDNA.

Bioinformatics, mapping, and data processing. Reads were mapped to the *T. brucei* 927 reference genome (version 5.2) by using bowtie (69, 70). Contaminating rRNA reads were removed computationally. Details are provided in the supplemental material. All scripts used in this study will be provided upon request. For RNA-Seq, biological replicates were prepared for input and RIP RNAs. Both Spearman's rank correlation and Pearson's product-moment correlation were 0.94, with a P value of $<2.2e{-}16$. For rrm1 RNAi analysis, SLT was performed once each for induced and uninduced cultures. Biological replicates were tested by qRT-PCR and showed concordance for the 12 genes tested.

ChIP. ChIP experiments were performed as described previously (71, 72) with minor modifications (see the supplemental material). One-nanogram amounts of total ChIP and input DNA were added to each reaction mixture; qPCRs were performed in triplicate. Primers used for qPCR are listed in the supplemental material.

Stress conditions. To study the effect of stress on the localization of TbRRM1, procyclic forms were incubated for 1 h under the following conditions: heat shock at 41°C, as described by Kramer et al. (52), starvation in PBS, genotoxic stress with 10 mM hydroxurea or 100 μM methyl-methane sulfonate (MMS), osmotic stress with 600 mM sorbitol, ER stress with 5 μM arsenite or 50 μg/ml cycloheximide, and transcription arrest with 50 μg/ml actinomycin D. Following incubation, cells were washed and processed for fluorescence microscopy.

SUPPLEMENTAL MATERIAL

Supplemental material for this article may be found at http://mbio.asm.org/lookup/suppl/doi:10.1128/mBio.00114-15/-/DCSupplemental.

Text S1, PDF file, 0.1 MB.
Figure S1, PDF file, 0.2 MB.
Figure S2, PDF file, 0.5 MB.
Figure S3, PDF file, 0.2 MB.
Figure S4, PDF file, 0.8 MB.
Figure S5, PDF file, 0.1 MB.
Table S1, XLS file, 0.7 MB.
Table S2, XLSX file, 0.6 MB.

ACKNOWLEDGMENTS

REFERENCES

1. **Fernández-Moya SM, Estévez AM**. 2010. Posttranscriptional control and the role of RNA-binding proteins in gene regulation in trypanosomatid protozoan parasites. RNA **1:**34–46. http://dx.doi.org/10.1002/wrna.6.

2. **De Gaudenzi J, Frasch AC, Clayton C**. 2005. RNA-binding domain proteins in kinetoplastids: a comparative analysis. Eukaryot Cell **4:**2106–2114. http://dx.doi.org/10.1128/EC.4.12.2106-2114.2005.

3. **Preusser C, Jaé N, Bindereif A**. 2012. mRNA splicing in trypanosomes. Int J Med Microbiol **302:**221–224. http://dx.doi.org/10.1016/j.ijmm.2012.07.004.

4. **Flück C, Salomone JY, Kurath U, Roditi I**. 2003. Cycloheximide-mediated accumulation of transcripts from a procyclin expression site depends on the intergenic region. Mol Biochem Parasitol **127:**93–97. http://dx.doi.org/10.1016/S0166-6851(02)00310-9.

5. **Stern MZ, Gupta SK, Salmon-Divon M, Haham T, Barda O, Levi S,** **Wachtel C, Nilsen TW, Michaeli S**. 2009. Multiple roles for polypyrimidine tract binding (PTB) proteins in trypanosome RNA metabolism. RNA **15:**648–665. http://dx.doi.org/10.1261/rna.1230209.

6. **Schwede A, Kramer S, Carrington M**. 2012. How do trypanosomes change gene expression in response to the environment? Protoplasma **249:**223–238. http://dx.doi.org/10.1007/s00709-011-0282-5.

7. **Engstler M, Boshart M**. 2004. Cold shock and regulation of surface protein trafficking convey sensitization to inducers of stage differentiation in *Trypanosoma brucei*. Genes Dev **18:**2798–2811. http://dx.doi.org/10.1101/gad.323404.

8. **Vassella E, Den Abbeele JV, Bütikofer P, Renggli CK, Furger A, Brun R, Roditi I**. 2000. A major surface glycoprotein of *Trypanosoma brucei* is expressed transiently during development and can be regulated post-transcriptionally by glycerol or hypoxia. Genes Dev **14:**615–626. http://dx.doi.org/10.1101/gad.14.5.615.

9. **Fernández-Moya SM, Carrington M, Estévez AM**. 2014. A short RNA stem-loop is necessary and sufficient for repression of gene expression during early logarithmic phase in trypanosomes. Nucleic Acids Res **42:**7201–7209. http://dx.doi.org/10.1093/nar/gku358.

10. **Urwyler S, Vassella E, Van Den Abbeele J, Renggli CK, Blundell P, Barry JD, Roditi I**. 2005. Expression of procyclin mRNAs during cyclical transmission of *Trypanosoma brucei*. PLoS Pathog **1:**e22. http://dx.doi.org/10.1371/journal.ppat.0010022.

11. **David M, Gabdank I, Ben-David M, Zilka A, Orr I, Barash D, Shapira M**. 2010. Preferential translation of Hsp83 in *Leishmania* requires a thermosensitive polypyrimidine-rich element in the 3′ UTR and involves scanning of the 5′ UTR. RNA **16:**364–374. doi:http://dx.doi.org/10.1261/rna.1874710.

12. **Archer SK, Luu VD, de Queiroz RA, Brems S, Clayton C**. 2009. Trypanosoma brucei PUF9 regulates mRNAs for proteins involved in replicative processes over the cell cycle. PLoS Pathog **5:**e1000565. http://dx.doi.org/10.1371/journal.ppat.1000565.

13. **Wurst M, Robles A, Po J, Luu VD, Brems S, Marentije M, Stoitsova S, Quijada L, Hoheisel J, Stewart M, Hartmann C, Clayton C**. 2009. An RNAi screen of the RRM-domain proteins of *Trypanosoma brucei*. Mol Biochem Parasitol **163:**61–65. http://dx.doi.org/10.1016/j.molbiopara.2008.09.001.

14. **Queiroz R, Benz C, Fellenberg K, Hoheisel JD, Clayton C**. 2009. Transcriptome analysis of differentiating trypanosomes reveals the existence of multiple post-transcriptional regulons. BMC Genomics **10:**495. http://dx.doi.org/10.1186/1471-2164-10-495.

15. **Walrad PB, Capewell P, Fenn K, Matthews KR**. 2012. The post-transcriptional *trans*-acting regulator, TbZFP3, co-ordinates transmission-stage enriched mRNAs in *Trypanosoma brucei*. Nucleic Acids Res **40:**2869–2883. http://dx.doi.org/10.1093/nar/gkr1106.

16. **Rudenko G, Bishop D, Gottesdiener K, Van der Ploeg LH**. 1989. Alpha-amanitin resistant transcription of protein coding genes in insect and bloodstream form Trypanosoma brucei. EMBO J **8:**4259–4263.

17. **Pays E, Coquelet H, Tebabi P, Pays A, Jefferies D, Steinert M, Koenig E, Williams RO, Roditi I**. 1990. *Trypanosoma brucei*: constitutive activity of the VSG and procyclin gene promoters. EMBO J **9:**3145–3151.

18. **Günzl A, Bruderer T, Laufer G, Schimanski B, Tu LC, Chung HM, Lee PT, Lee MG**. 2003. RNA polymerase I transcribes procyclin genes and variant surface glycoprotein gene expression sites in *Trypanosoma brucei*. Eukaryot Cell **2:**542–551. http://dx.doi.org/10.1128/EC.2.3.542-551.2003.

19. **Navarro M, Gull K**. 2001. A Pol I transcriptional body associated with VSG mono-allelic expression in *Trypanosoma brucei*. Nature **414:**759–763. http://dx.doi.org/10.1038/414759a.

20. **Landeira D, Navarro M**. 2007. Nuclear repositioning of the VSG promoter during developmental silencing in *Trypanosoma brucei*. J Cell Biol **176:**133–139. http://dx.doi.org/10.1083/jcb.200607174.

21. **Figueiredo LM, Cross GA**. 2010. Nucleosomes are depleted at the VSG expression site transcribed by RNA polymerase I in African trypanosomes. Eukaryot Cell **9:**148–154. http://dx.doi.org/10.1128/EC.00282-09.

22. **Stanne TM, Rudenko G**. 2010. Active VSG expression sites in *Trypanosoma brucei* are depleted of nucleosomes. Eukaryot Cell **9:**136–147. http://dx.doi.org/10.1128/EC.00281-09.

23. **Wang QP, Kawahara T, Horn D**. 2010. Histone deacetylases play distinct roles in telomeric VSG expression site silencing in African trypanosomes. Mol Microbiol **77:**1237–1245. http://dx.doi.org/10.1111/j.1365-2958.2010.07284.x.

24. **Siegel TN, Hekstra DR, Kemp LE, Figueiredo LM, Lowell JE, Fenyo D, Wang X, Dewell S, Cross GA**. 2009. Four histone variants mark the

boundaries of polycistronic transcription units in *Trypanosoma brucei*. Genes Dev **23**:1063–1076. http://dx.doi.org/10.1101/gad.1790409.

25. **Alexander R, Beggs JD.** 2010. Cross-talk in transcription, splicing and chromatin: who makes the first call? Biochem Soc Trans **38**:1251–1256. http://dx.doi.org/10.1042/BST0381251.

26. **Shukla S, Oberdoerffer S.** 2012. Co-transcriptional regulation of alternative pre-mRNA splicing. Biochim Biophys Acta **1819**:673–683. http://dx.doi.org/10.1016/j.bbagrm.2012.01.014.

27. **Kim S, Kim H, Fong N, Erickson B, Bentley DL.** 2011. Pre-mRNA splicing is a determinant of histone H3K36 methylation. Proc Natl Acad Sci U S A **108**:13564–13569. http://dx.doi.org/10.1073/pnas.1109475108.

28. **Morris SA, Shibata Y, Noma K, Tsukamoto Y, Warren E, Temple B, Grewal SI, Strahl BD.** 2005. Histone H3 K36 methylation is associated with transcription elongation in *Schizosaccharomyces pombe*. Eukaryot Cell **4**:1446–1454. http://dx.doi.org/10.1128/EC.4.8.1446-1454.2005.

29. **Krogan NJ, Kim M, Tong A, Golshani A, Cagney G, Krogan NJ, Kim M, Tong A, Golshani A, Cagney G, Canadien V, Richards DP, Beattie BK, Emili A, Boone C, Shilatifard A, Buratowski S, Greenblatt J.** 2003. Methylation of histone H3 by Set2 in *Saccharomyces cerevisiae* is linked to transcriptional elongation by RNA polymerase II. Mol Cell Biol **23**:4207–4218. http://dx.doi.org/10.1128/MCB.23.12.4207-4218.2003.

30. **Batsché E, Yaniv M, Muchardt C.** 2006. The human SWI/SNF subunit Brm is a regulator of alternative splicing. Nat Struct Mol Biol **13**:22–29. http://dx.doi.org/10.1038/nsmb1030.

31. **Brody Y, Neufeld N, Bieberstein N, Causse SZ, Böhnlein EM, Neugebauer KM, Darzacq X, Shav-Tal Y.** 2011. The in vivo kinetics of RNA polymerase II elongation during co-transcriptional splicing. PLoS Biol **9**:e1000573. http://dx.doi.org/10.1371/journal.pbio.1000573.

32. **Sapra AK, Ankö ML, Grishina I, Lorenz M, Pabis M, Poser I, Rollins J, Weiland EM, Neugebauer KM.** 2009. SR protein family members display diverse activities in the formation of nascent and mature mRNPs in vivo. Mol Cell **34**:179–190. http://dx.doi.org/10.1016/j.molcel.2009.02.031.

33. **Lin S, Coutinho-Mansfield G, Wang D, Pandit S, Fu XD.** 2008. The splicing factor SC35 has an active role in transcriptional elongation. Nat Struct Mol Biol **15**:819–826. http://dx.doi.org/10.1038/nsmb.1461.

34. **Manger ID, Boothroyd JC.** 1998. Identification of a nuclear protein in *Trypanosoma brucei* with homology to RNA-binding proteins from cis-splicing systems. Mol Biochem Parasitol **97**:1–11. http://dx.doi.org/10.1016/S0166-6851(98)00118-2.

35. **Ismaïli N, Pérez-Morga D, Walsh P, Mayeda A, Pays A, Tebabi P, Krainer AR, Pays E.** 1999. Characterization of a SR protein from *Trypanosoma brucei* with homology to RNA-binding cis-splicing proteins. Mol Biochem Parasitol **102**:103–115. http://dx.doi.org/10.1016/S0166-6851(99)00091-2.

36. **Gupta SK, Chikne V, Eliaz D, Tkacz ID, Naboishchikov I, Carmi S, Waldman Ben-Asher H, Michaeli S.** 2014. Two splicing factors carrying serine–arginine motifs, TSR1 and TSR1IP, regulate splicing, mRNA stability, and rRNA processing in *Trypanosoma brucei*. RNA Biol **11**:715–731. http://dx.doi.org/10.4161/rna.29143.

37. **Juge F, Fernando C, Fic W, Tazi J.** 2010. The SR protein B52/SRp55 is required for DNA topoisomerase I recruitment to chromatin, mRNA release and transcription shutdown. PLOS Genet **6**:e1001124. http://dx.doi.org/10.1371/journal.pgen.1001124.

38. **Manger ID, Boothroyd JC.** 2001. Targeted disruption of an essential RNA-binding protein perturbs cell division in *Trypanosoma brucei*. Mol Biochem Parasitol **116**:239–245. http://dx.doi.org/10.1016/S0166-6851(01)00322-X.

39. **Luz Ambrósio D, Lee JH, Panigrahi AK, Nguyen TN, Cicarelli RM, Günzl A.** 2009. Spliceosomal proteomics in Trypanosoma brucei *reveal new RNA splicing factors. Eukaryot Cell **8**:990–1000. http://dx.doi.org/10.1128/EC.00075-09.

40. **Preusser C, Palfi Z, Bindereif A.** 2009. Special Sm core complex functions in assembly of the U2 small nuclear ribonucleoprotein of *Trypanosoma brucei*. Eukaryot Cell **8**:1228–1234. http://dx.doi.org/10.1128/EC.00090-09.

41. **Wurst M, Seliger B, Jha BA, Klein C, Queiroz R, Clayton C.** 2012. Expression of the RNA recognition motif protein RBP10 promotes a bloodstream-form transcript pattern in *Trypanosoma brucei*. Mol Microbiol **83**:1048–1063. http://dx.doi.org/10.1111/j.1365-2958.2012.07988.x.

42. **Bringaud F, Biteau N, Melville SE, Hez S, El-Sayed NM, Leech V, Berriman M, Hall N, Donelson JE, Baltz T.** 2002. A new, expressed multigene family containing a hot spot for insertion of retroelements is associated with polymorphic subtelomeric regions of *Trypanosoma brucei*. Eukaryot Cell **1**:137–151. http://dx.doi.org/10.1128/EC.1.1.137-151.2002.

43. **Telleria EL, Benoit JB, Zhao X, Savage AF, Regmi S, Alves e Silva TL, O'Neill M, Aksoy S.** 2014. Insights into the trypanosome-host interactions revealed through transcriptomic analysis of parasitized tsetse fly salivary glands. PLoS Negl Trop Dis **8**:e2649. http://dx.doi.org/10.1371/journal.pntd.0002649.

44. **Chaudhuri M, Ajayi W, Temple S, Hill GC.** 1995. Identification and partial purification of a stage-specific 33-kDa mitochondrial protein as the alternative oxidase of the *Trypanosoma brucei brucei* bloodstream trypomastigotes. J Eukaryot Microbiol **42**:467–472. http://dx.doi.org/10.1111/j.1550-7408.1995.tb05892.x.

45. **Vanhollebeke B, De Muylder G, Nielsen MJ, Pays A, Tebabi P, Dieu M, Raes M, Moestrup SK, Pays E.** 2008. A haptoglobin-hemoglobin receptor conveys innate immunity to *Trypanosoma brucei* in humans. Science **320**:677–681. http://dx.doi.org/10.1126/science.1156296.

46. **Ziegelbauer K, Overath P.** 1992. Identification of invariant surface glycoproteins in the bloodstream stage of *Trypanosoma brucei*. J Biol Chem **267**:10791–10796.

47. **Urwyler S, Studer E, Renggli CK, Roditi I.** 2007. A family of stage-specific alanine-rich proteins on the surface of epimastigote forms of *Trypanosoma brucei*. Mol Microbiol **63**:218–228. http://dx.doi.org/10.1111/j.1365-2958.2006.05492.x.

48. **Mani J, Güttinger A, Schimanski B, Heller M, Acosta-Serrano A, Pescher P, Späth G, Roditi I.** 2011. Alba-domain proteins of *Trypanosoma brucei* are cytoplasmic RNA-binding proteins that interact with the translation machinery. PLoS One **6**:e22463. http://dx.doi.org/10.1371/journal.pone.0022463.

49. **Roditi I, Carrington M, Turner M.** 1987. Expression of a polypeptide containing a dipeptide repeat is confined to the insect stage of *Trypanosoma brucei*. Nature **325**:272–274. http://dx.doi.org/10.1038/325272a0.

50. **Fragoso CM, Schumann Burkard G, Oberle M, Renggli CK, Hilzinger K, Roditi I.** 2009. PSSA-2, a membrane-spanning phosphoprotein of *Trypanosoma brucei*, is required for efficient maturation of infection. PLoS One **4**:e7074. http://dx.doi.org/10.1371/journal.pone.0007074.

51. **Mayho M, Fenn K, Craddy P, Crosthwaite S, Matthews K.** 2006. Post-transcriptional control of nuclear-encoded cytochrome oxidase subunits in *Trypanosoma brucei*: evidence for genome-wide conservation of life-cycle stage-specific regulatory elements. Nucleic Acids Res **34**:5312–5324. http://dx.doi.org/10.1093/nar/gkl598.

52. **Kramer S, Queiroz R, Ellis L, Webb H, Hoheisel JD, Clayton C, Carrington M.** 2008. Heat shock causes a decrease in polysomes and the appearance of stress granules in trypanosomes independently of eIF2α phosphorylation at Thr169. J Cell Sci **121**:3002–3014. http://dx.doi.org/10.1242/jcs.031823.

53. **Nilsson D, Gunasekera K, Mani J, Osteras M, Farinelli L, Baerlocher L, Roditi I, Ochsenreiter T.** 2010. Spliced leader trapping reveals widespread alternative splicing patterns in the highly dynamic transcriptome of *Trypanosoma brucei*. PLoS Pathog **6**:e1001037. http://dx.doi.org/10.1371/journal.ppat.1001037.

54. **Pellé R, Murphy NB.** 1993. Stage-specific differential polyadenylation of mini-exon derived RNA in African trypanosomes. Mol Biochem Parasitol **59**:277–286. http://dx.doi.org/10.1016/0166-6851(93)90225-M.

55. **Pedrotti S, Busà R, Compagnucci C, Sette C.** 2012. The RNA recognition motif protein RBM11 is a novel tissue-specific splicing regulator. Nucleic Acids Res **40**:1021–1032. http://dx.doi.org/10.1093/nar/gkr819.

56. **Twyffels L, Gueydan C, Kruys V.** 2011. Shuttling SR proteins: more than splicing factors. FEBS J **278**:3246–3255. http://dx.doi.org/10.1111/j.1742-4658.2011.08274.x.

57. **Kelly S, Kramer S, Schwede A, Maini PK, Gull K, Carrington M.** 2012. Genome organization is a major component of gene expression control in response to stress and during the cell division cycle in trypanosomes. Open Biol **2**:120033. http://dx.doi.org/10.1098/rsob.120033.

58. **Zhong XY, Wang P, Han J, Rosenfeld MG, Fu XD.** 2009. SR proteins in vertical integration of gene expression from transcription to RNA processing to translation. Mol Cell **35**:1–10. http://dx.doi.org/10.1016/j.molcel.2009.06.016.

59. **Batista PJ, Chang HY.** 2013. Long noncoding RNAs: cellular address codes in development and disease. Cell **152**:1298–1307. http://dx.doi.org/10.1016/j.cell.2013.02.012.

60. **Jha BA, Fadda A, Merce C, Mugo E, Droll D, Clayton C.** 2014. Depletion of the *trypanosome Pumilio* domain protein PUF2 or of some other essen-

tial proteins causes transcriptome changes related to coding region length. Eukaryot Cell **13**:664–674. http://dx.doi.org/10.1128/EC.00018-14.

61. **Le Ray D, Barry JD, Easton C, Vickerman K**. 1977. First tsetse fly transmission of the "AnTat" serodeme of *Trypanosoma brucei*. Ann Soc Belg Med Trop **57**:369–381.

62. **Brun R, Schönenberger**. 1979. Cultivation and *in vitro* cloning or procyclic culture forms of *Trypanosoma brucei* in a semi-defined medium. Acta Trop **36**:289–292.

63. **Roditi I, Schwarz H, Pearson TW, Beecroft RP, Liu MK, Richardson JP, Bühring HJ, Pleiss J, Bülow R, Williams RO, Overathh P**. 1989. Procyclin gene expression and loss of the variant surface glycoprotein during differentiation of *Trypanosoma brucei*. J Cell Biol **108**:737–746. http://dx.doi.org/10.1083/jcb.108.2.737.

64. **Haenni S, Renggli CK, Fragoso CM, Oberle M, Roditi I**. 2006. The procyclin-associated genes of *Trypanosoma brucei* are not essential for cyclical transmission by tsetse. Mol Biochem Parasitol **150**:144–156. http://dx.doi.org/10.1016/j.molbiopara.2006.07.005.

65. **Ruepp S, Furger A, Kurath U, Renggli CK, Hemphill A, Brun R, Roditi I**. 1997. Survival of *Trypanosoma brucei* in the tsetse fly is enhanced by the expression of specific forms of procyclin. J Cell Biol **137**:1369–1379. http://dx.doi.org/10.1083/jcb.137.6.1369.

66. **Schumann Burkard G, Käser S, de Araújo PR, Schimanski B, Naguleswaran A, Knüsel S, Heller M, Roditi I**. 2013. Nucleolar proteins regulate stage-specific gene expression and ribosomal RNA maturation in *Trypanosoma brucei*. Mol Microbiol **88**:827–840. http://dx.doi.org/10.1111/mmi.12227.

67. **Wessel D, Flügge UI**. 1984. A method for the quantitative recovery of protein in dilute solution in the presence of detergents and lipids. Anal Biochem **138**:141–143. http://dx.doi.org/10.1016/0003-2697(84)90782-6.

68. **Al Kaabi A, Traupe T, Stutz M, Buchs N, Heller M**. 2012. Cause or effect of arteriogenesis: compositional alterations of microparticles from CAD patients undergoing external counterpulsation therapy. PLoS One **7**:e46822. http://dx.doi.org/10.1371/journal.pone.0046822.

69. **Langmead B, Trapnell C, Pop M, Salzberg SL**. 2009. Ultrafast and memory-efficient alignment of short DNA sequences to the human genome. Genome Biol **10**:R25. http://dx.doi.org/10.1186/gb-2009-10-3-r25.

70. **Li H, Durbin R**. 2009. Fast and accurate short read alignment with burrows-Wheeler transform. Bioinformatics **25**:1754–1760. http://dx.doi.org/10.1093/bioinformatics/btp324.

71. **Lowell JE, Cross GA**. 2004. A variant histone H3 is enriched at telomeres in *Trypanosoma brucei*. J Cell Sci **117**:5937–5947. http://dx.doi.org/10.1242/jcs.01515.

72. **Dahl JA, Collas P**. 2007. A quick and quantitative chromatin immunoprecipitation assay for small cell samples. Front Biosci **12**:4925–4931. http://dx.doi.org/10.2741/2438.